SUPPORTING INFORMATION

A route to aliphatic poly(ester)s with thiol pendant groups: from monomer design to editable porous scaffolds

Tiziana Fuoco,[§,†] *Anna Finne-Wistrand,*[†] *Daniela Pappalardo**[‡,†]

† Department of Fibre and Polymer Technology, KTH Royal Institute of Technology, Stockholm, Sweden

‡ Department of Science and Technology, University of Sannio, via dei Mulini 59/A, 82100 Benevento, Italy

§ Department of Chemistry and Biology "A. Zambelli", University of Salerno, via Giovanni Paolo II 132, 84084 Fisciano (SA), Italy

E-mail: pappalardo@unisannio.it

TABLE OF CONTENTS

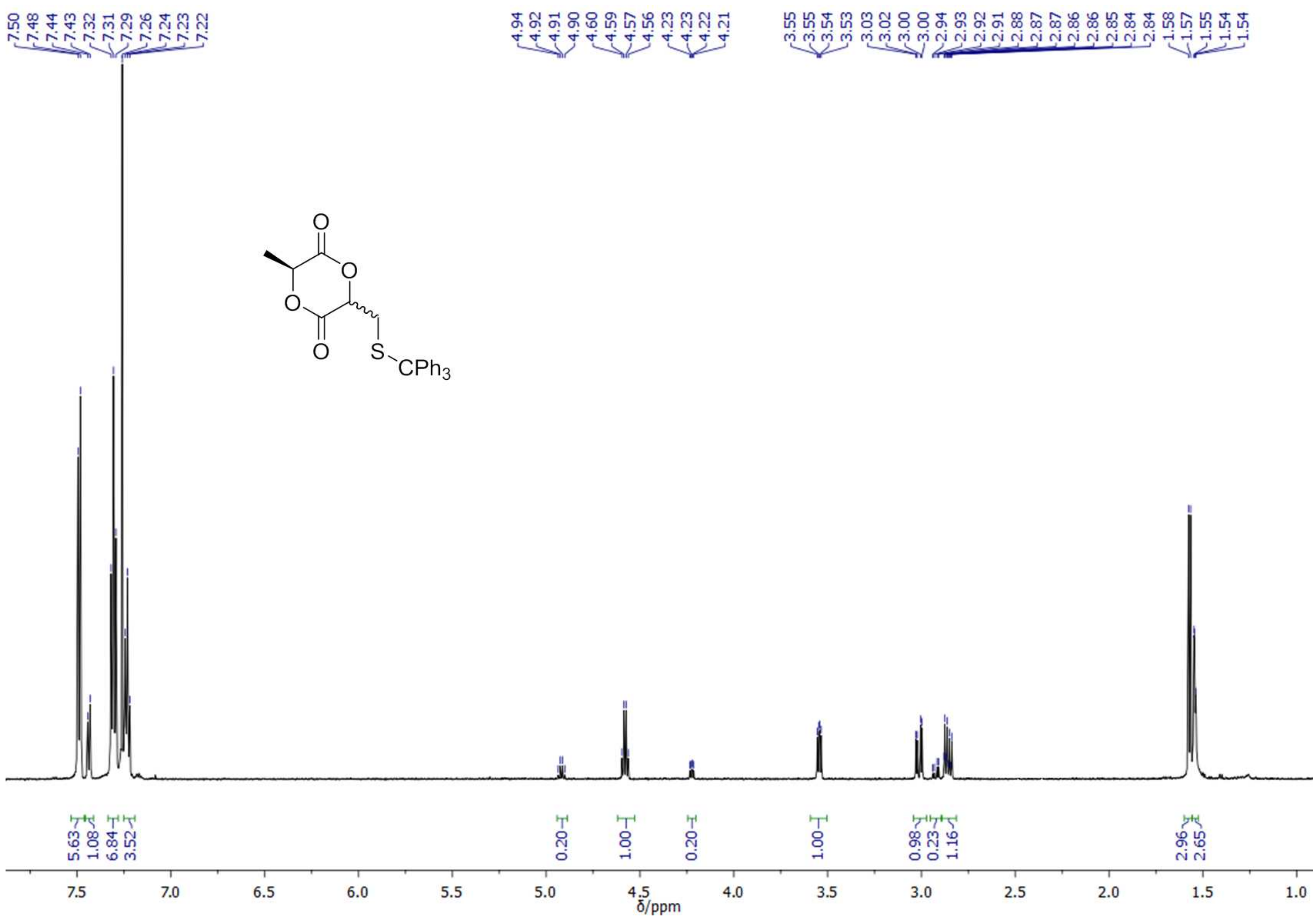

Figure S1. [1]H NMR (600 MHz, $CDCl_3$, RT) of the diastereisomeric mixture of 3-methyl-6-(tritylthiomethyl)-1,4-dioxane-2,5-dione.

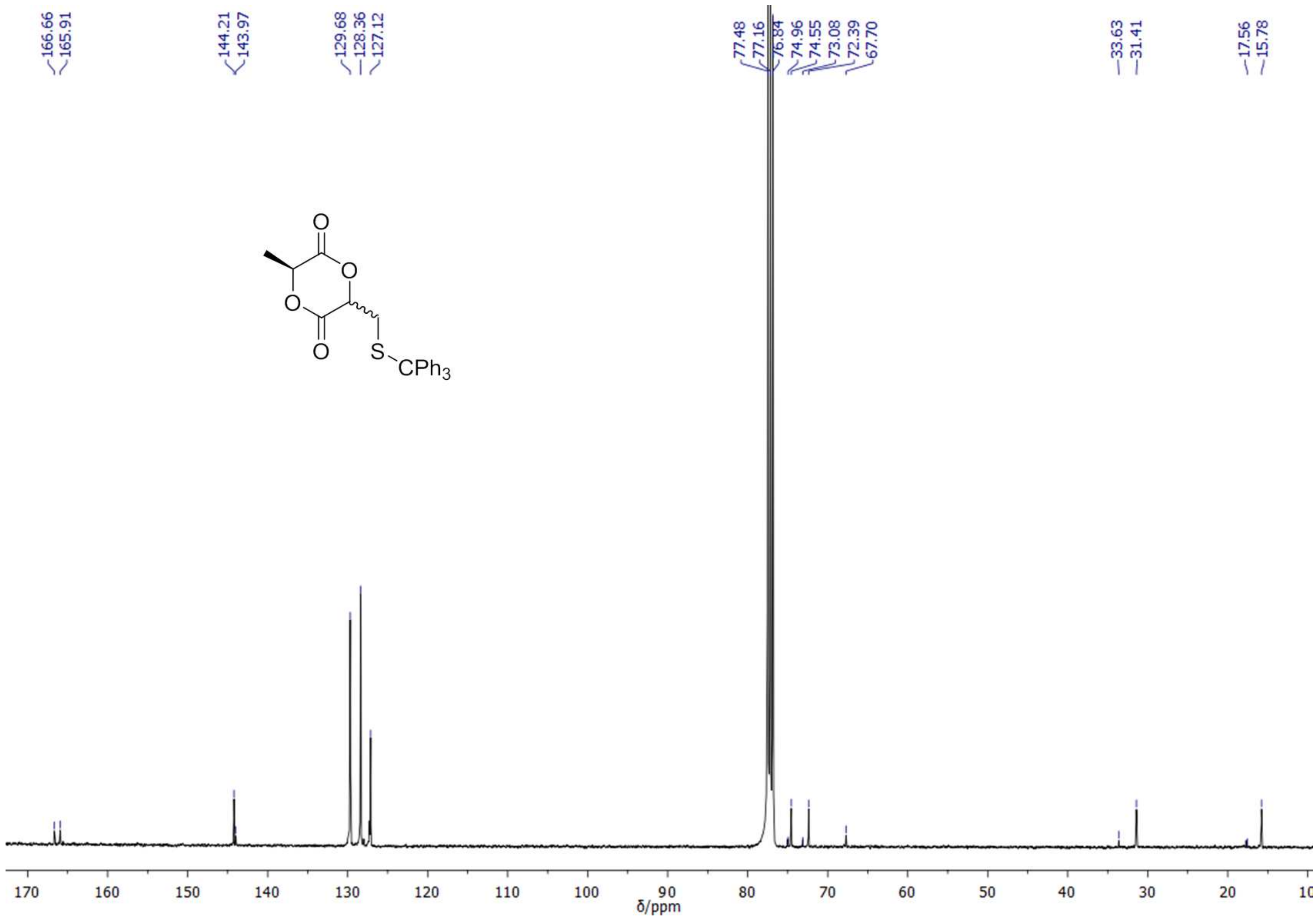

Figure S2. ^{13}C NMR (100 MHz, $CDCl_3$, RT) of the diastereisomeric mixture of 3-methyl-6-(tritylthiomethyl)-1,4-dioxane-2,5-dione.

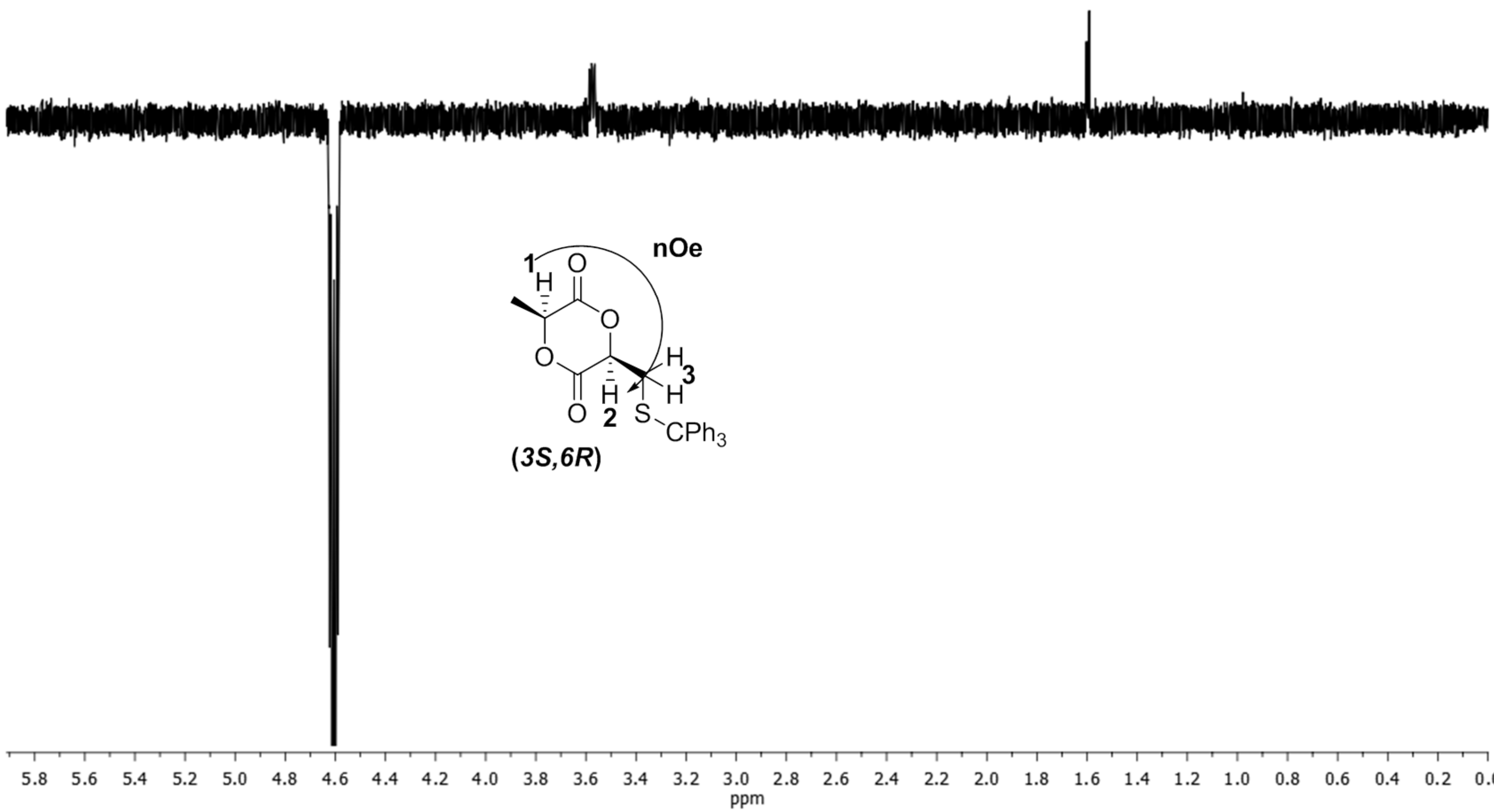

Figure S3. NOE ^{1}H NMR (100 MHz, $CDCl_3$, RT) of the diastereisomeric mixture of 3-methyl-6-(tritylthiomethyl)-1,4-dioxane-2,5-dione.

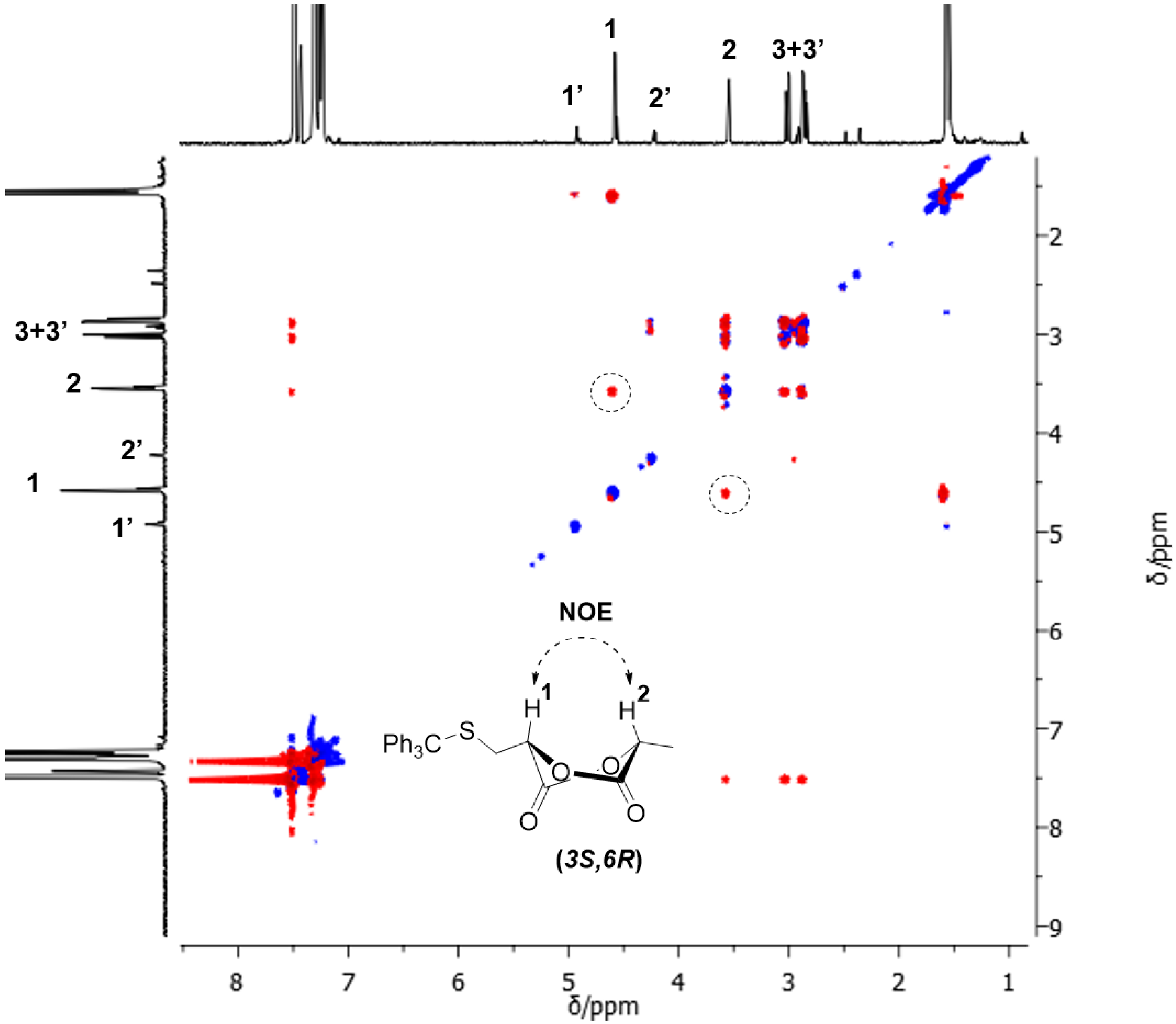

Figure S4. ^{1}H NOESY NMR (600 MHz, $CDCl_3$, RT) of the diastereisomeric mixture of 3-methyl-6-(tritylthiomethyl)-1,4-dioxane-2,5-dione.

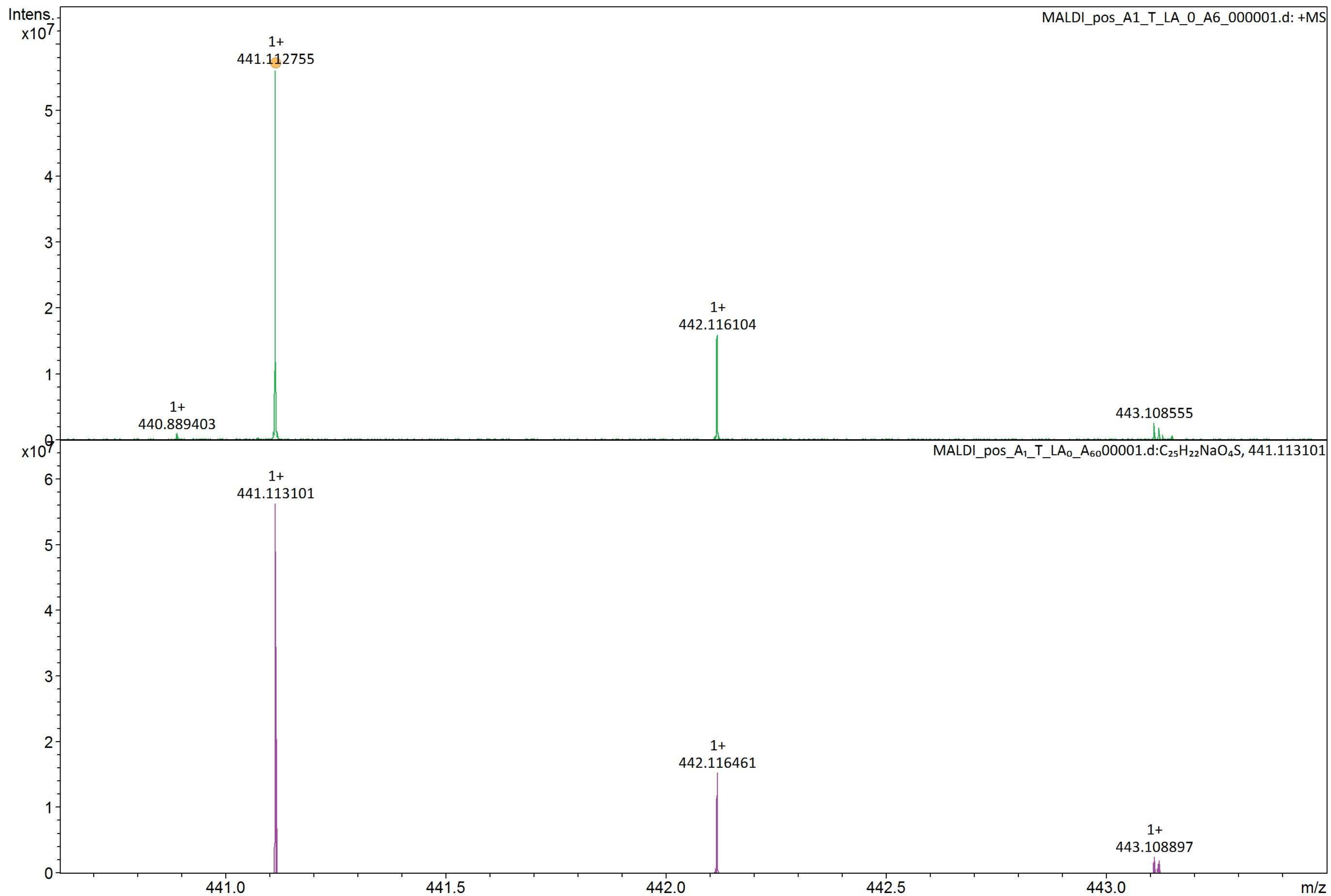

Figure S5. HR-MS MALDI of 3-methyl-6-(tritylthiomethyl)-1,4-dioxane-2,5-dione.

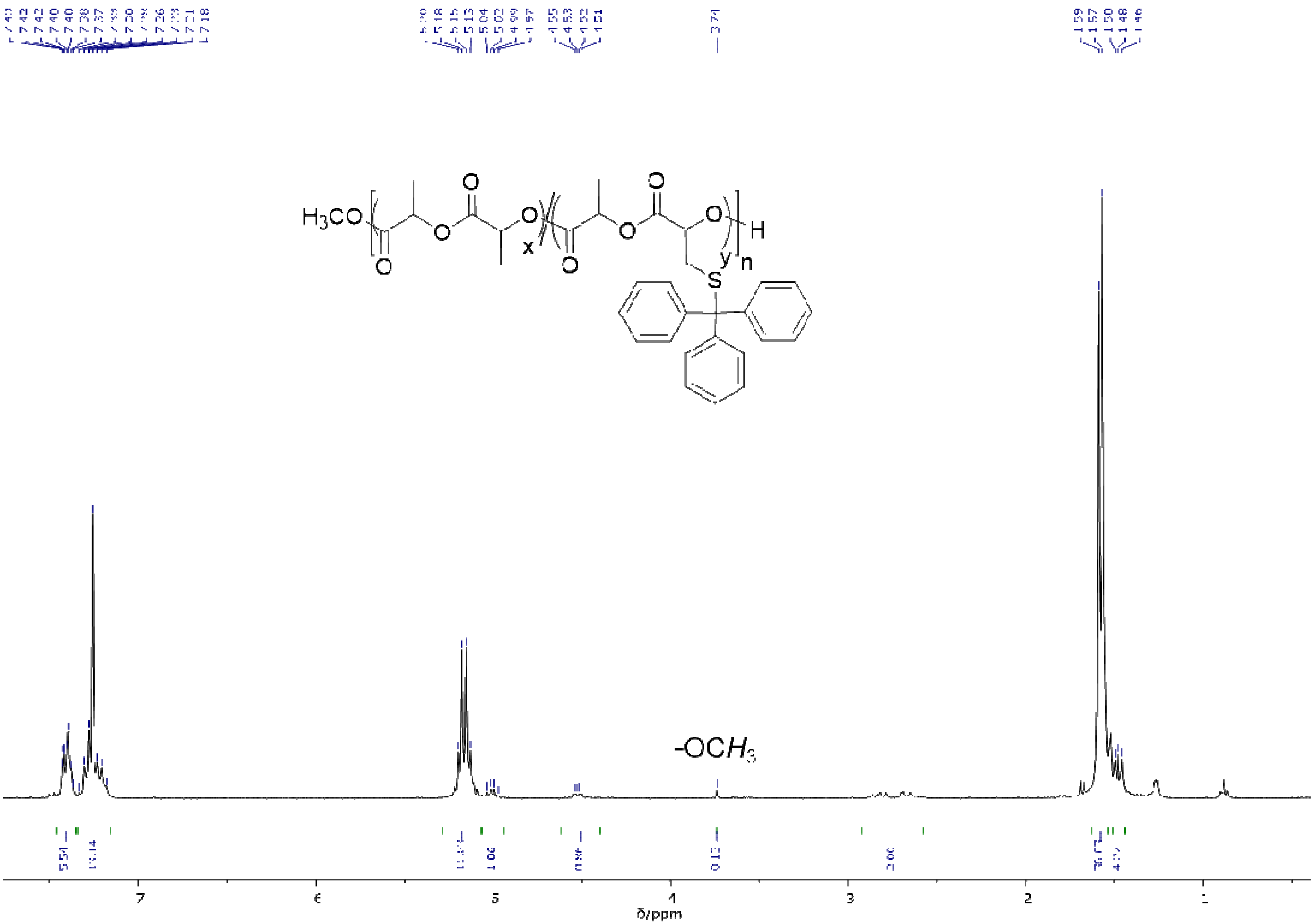

Figure S6. [1]H NMR (400 MHz, $CDCl_3$, RT) of poly[(TrtS–LA)-*co*-LA] (sample **a**).

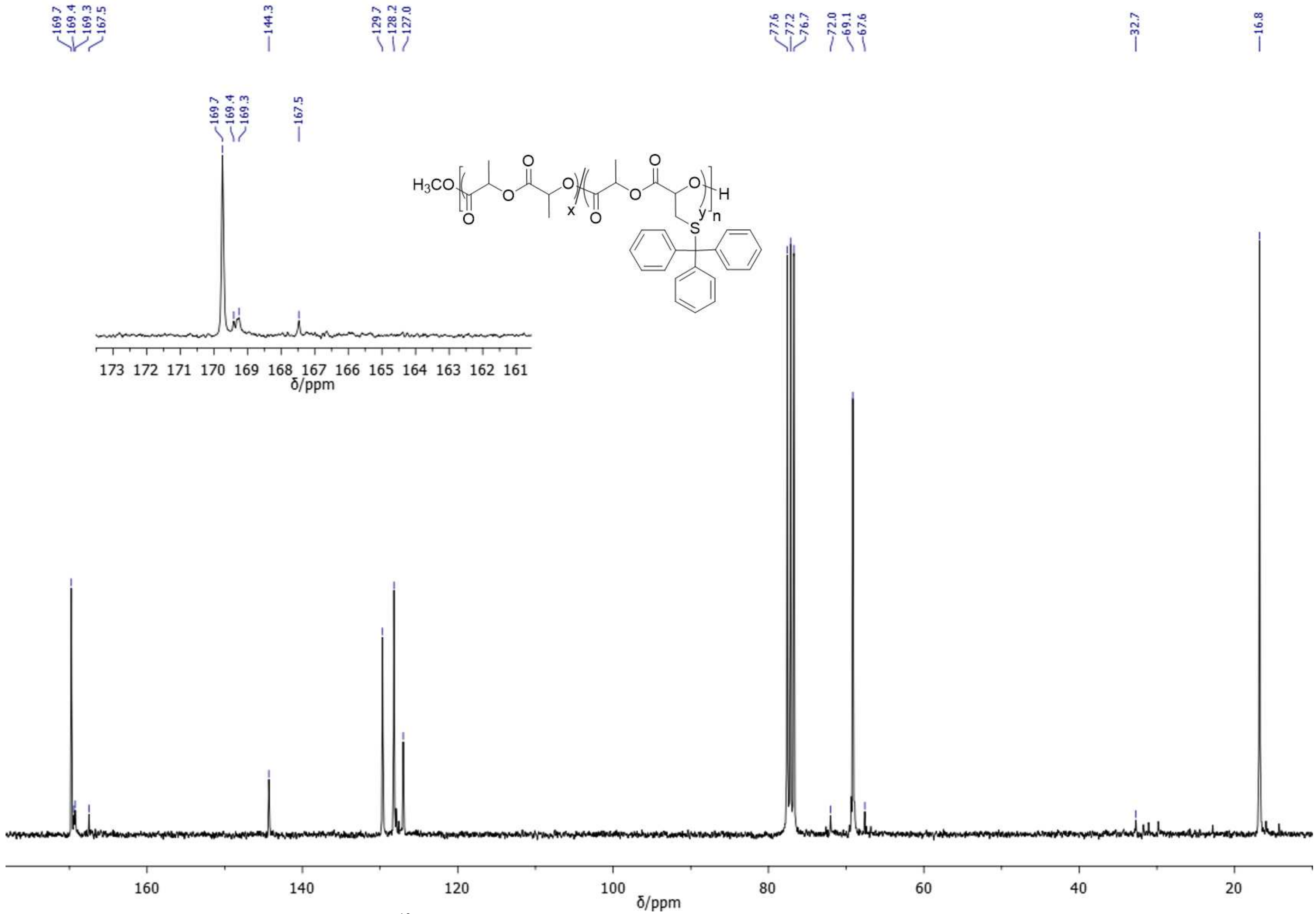

Figure S7. ^{13}C NMR (75 MHz, $CDCl_3$, RT) of poly[(TrtS–LA)-*co*-LA] (sample **a**).

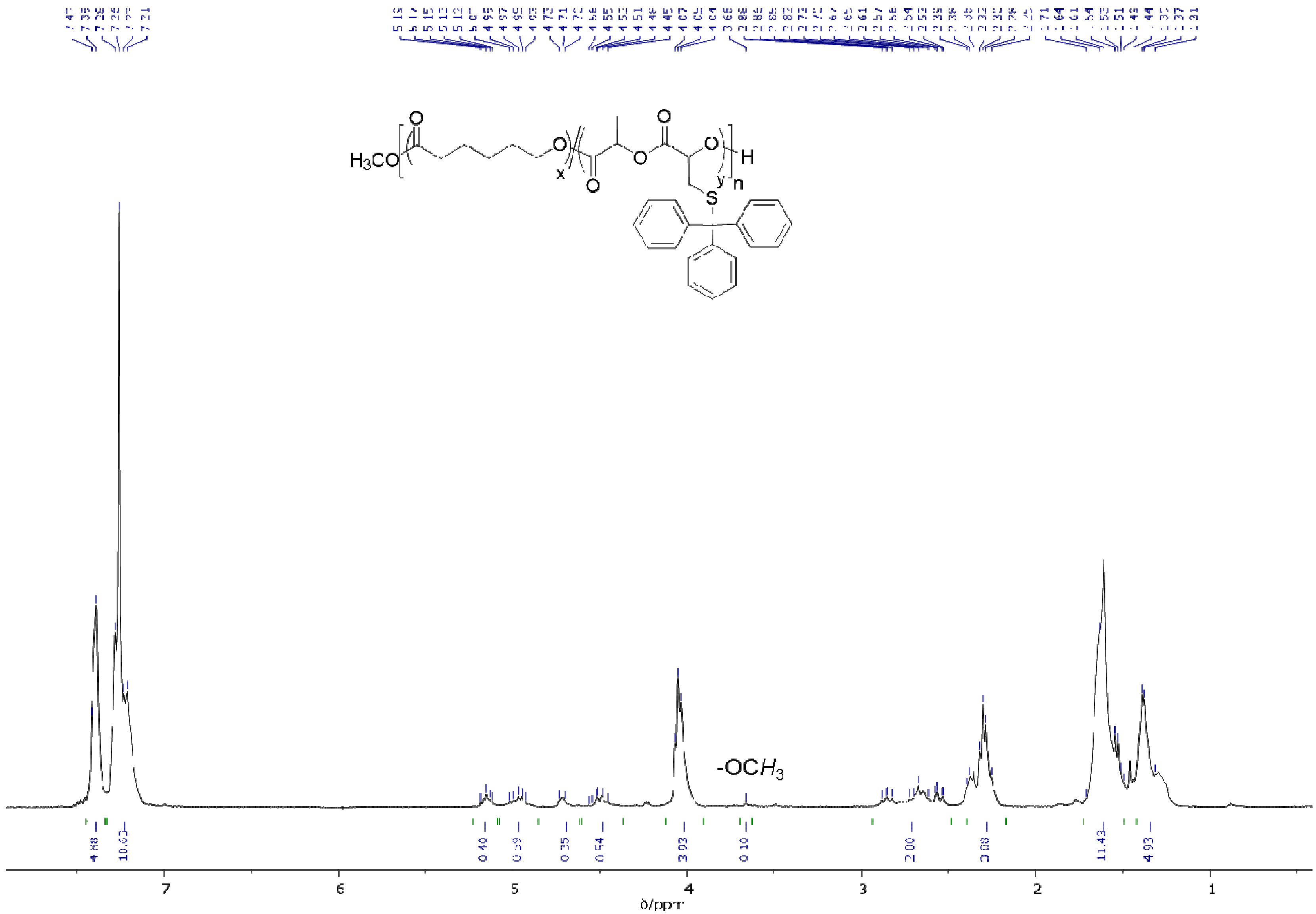

Figure S8. ^{1}H NMR (400 MHz, $CDCl_3$, RT) of poly[(TrtS–LA)-*co*-CL] (sample **b**).

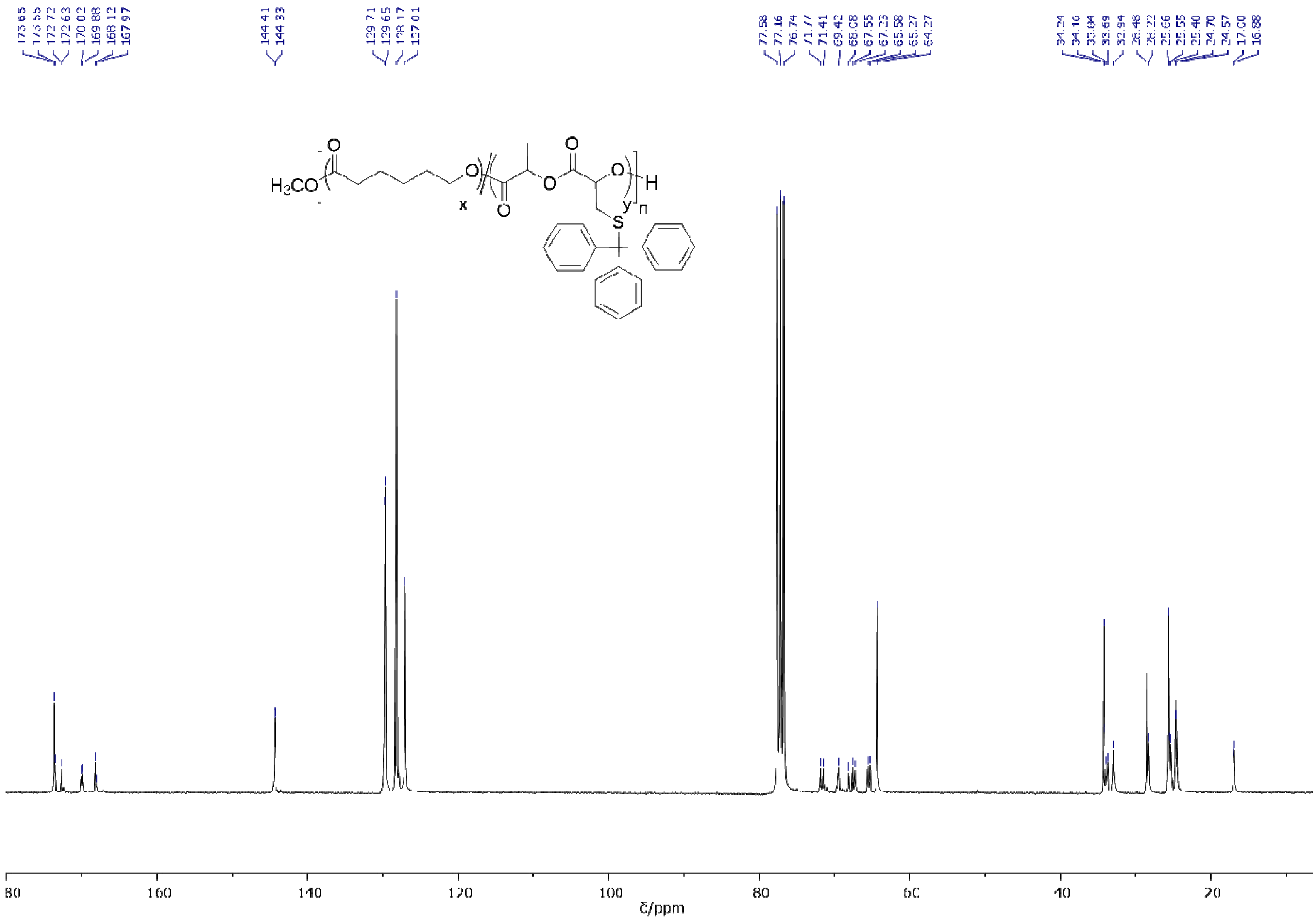

Figure S9. ^{13}C NMR (75 MHz, $CDCl_3$, RT) of poly[(TrtS–LA)-*co*-CL] (sample **b**).

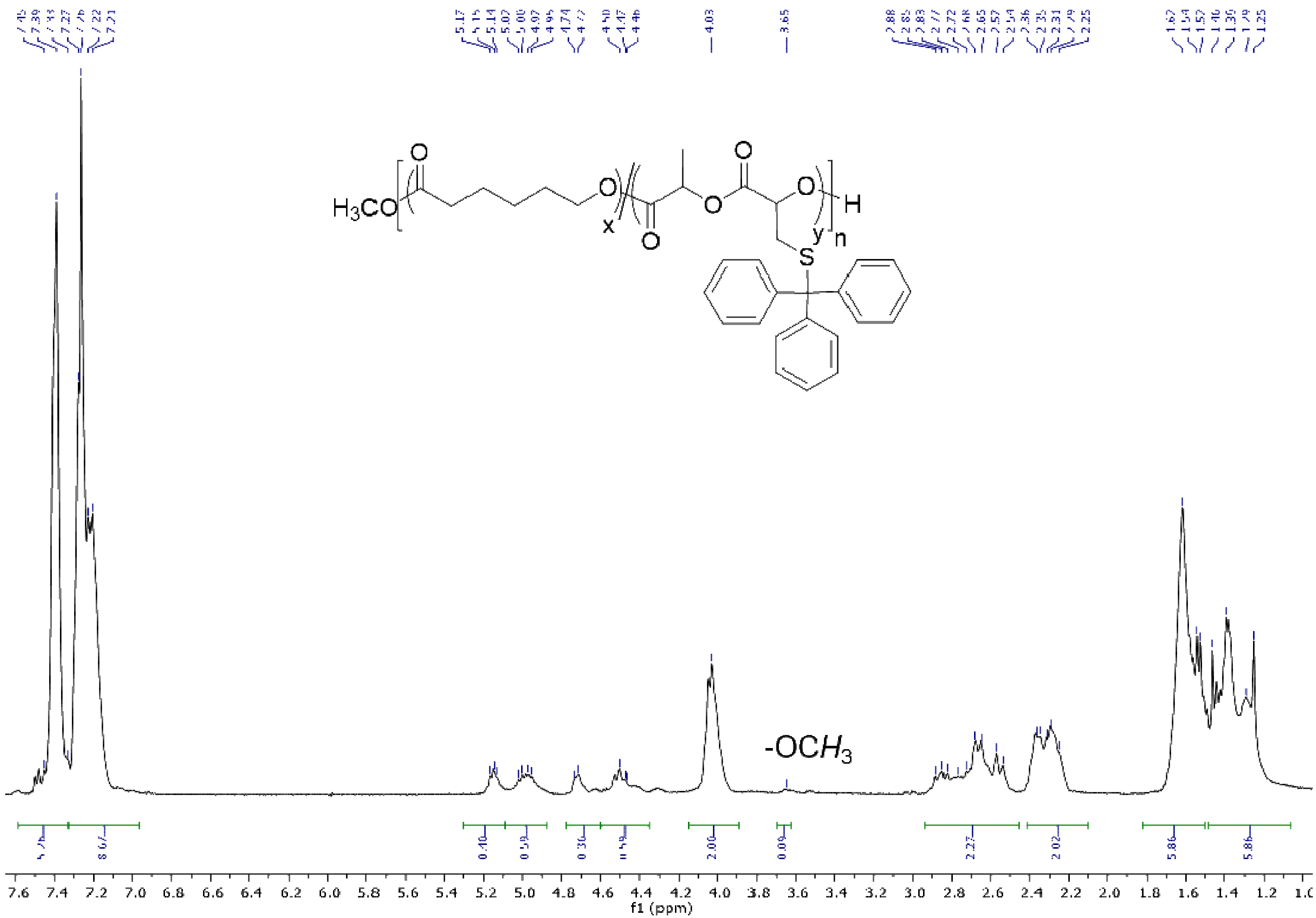

Figure S10. ^{13}H NMR (300 MHz, $CDCl_3$, RT) of poly[(TrtS–LA)-*co*-CL] (sample **b'**).

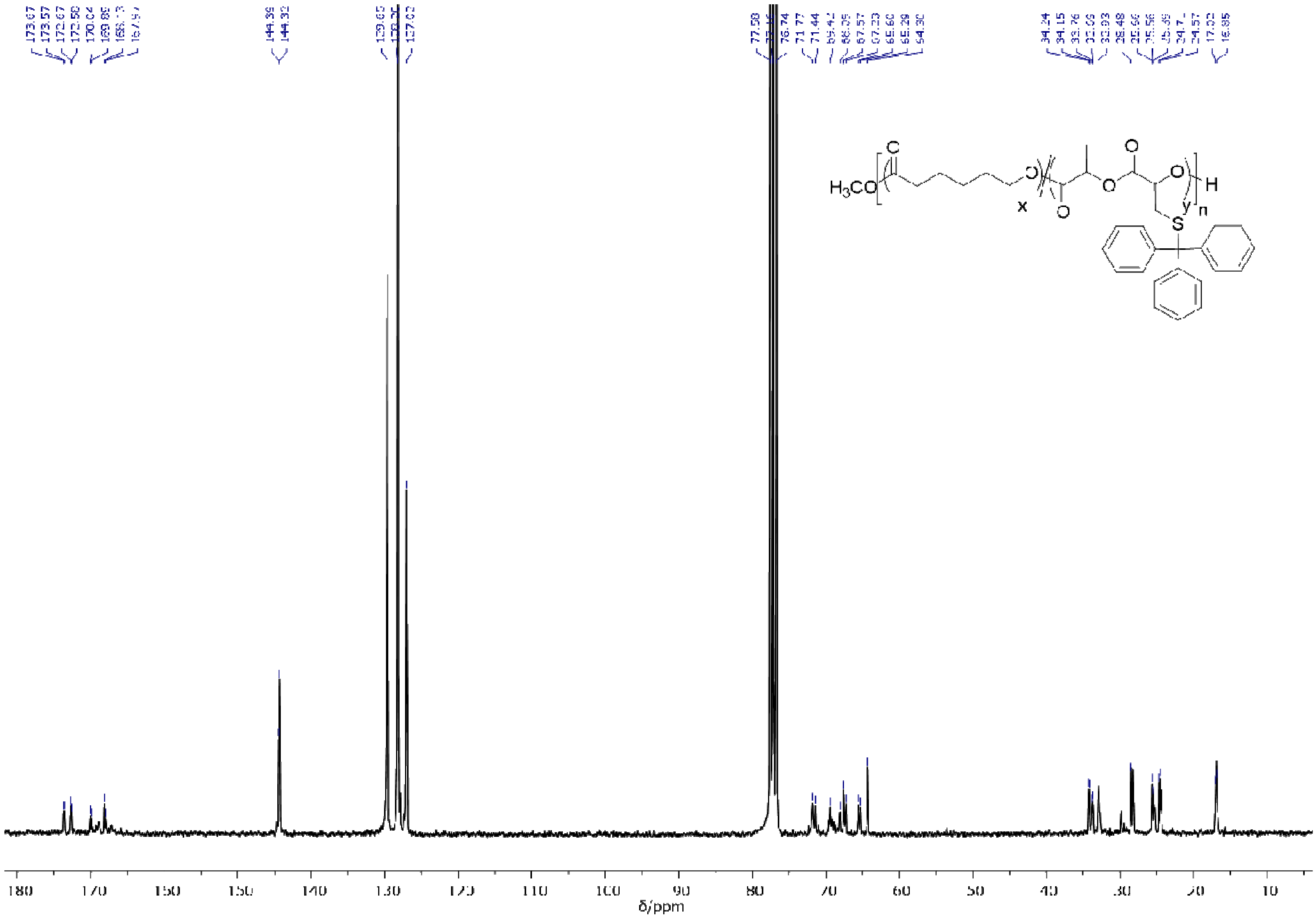

Figure S11. ^{13}C NMR (75 MHz, $CDCl_3$, RT) of poly[(TrtS–LA)-*co*-CL] (sample **b'**).

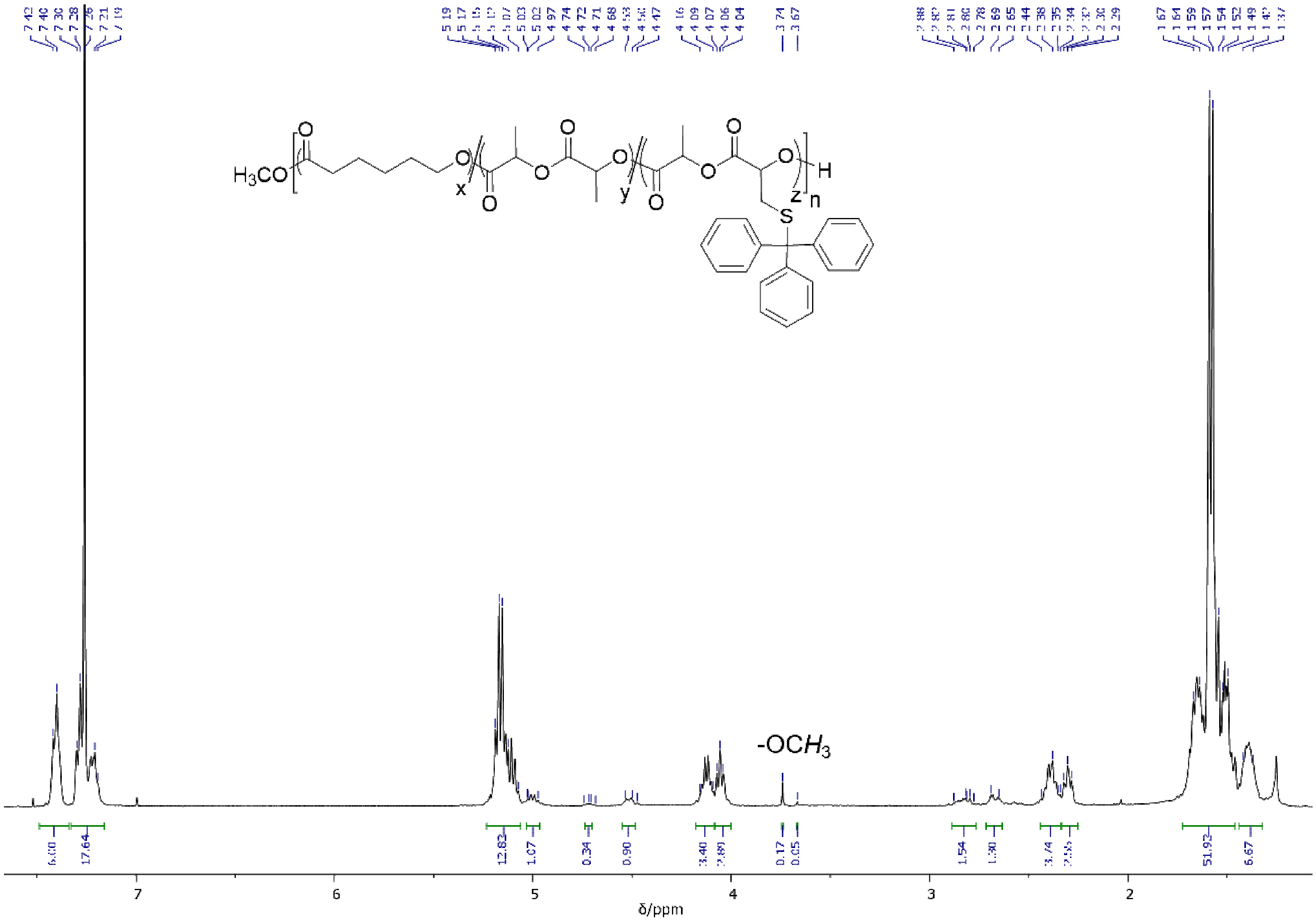

Figure S12. ^{1}H NMR (400 MHz, $CDCl_3$, RT) of poly[(TrtS–LA)-*co*-CL-*co*-LA] (sample **c**).

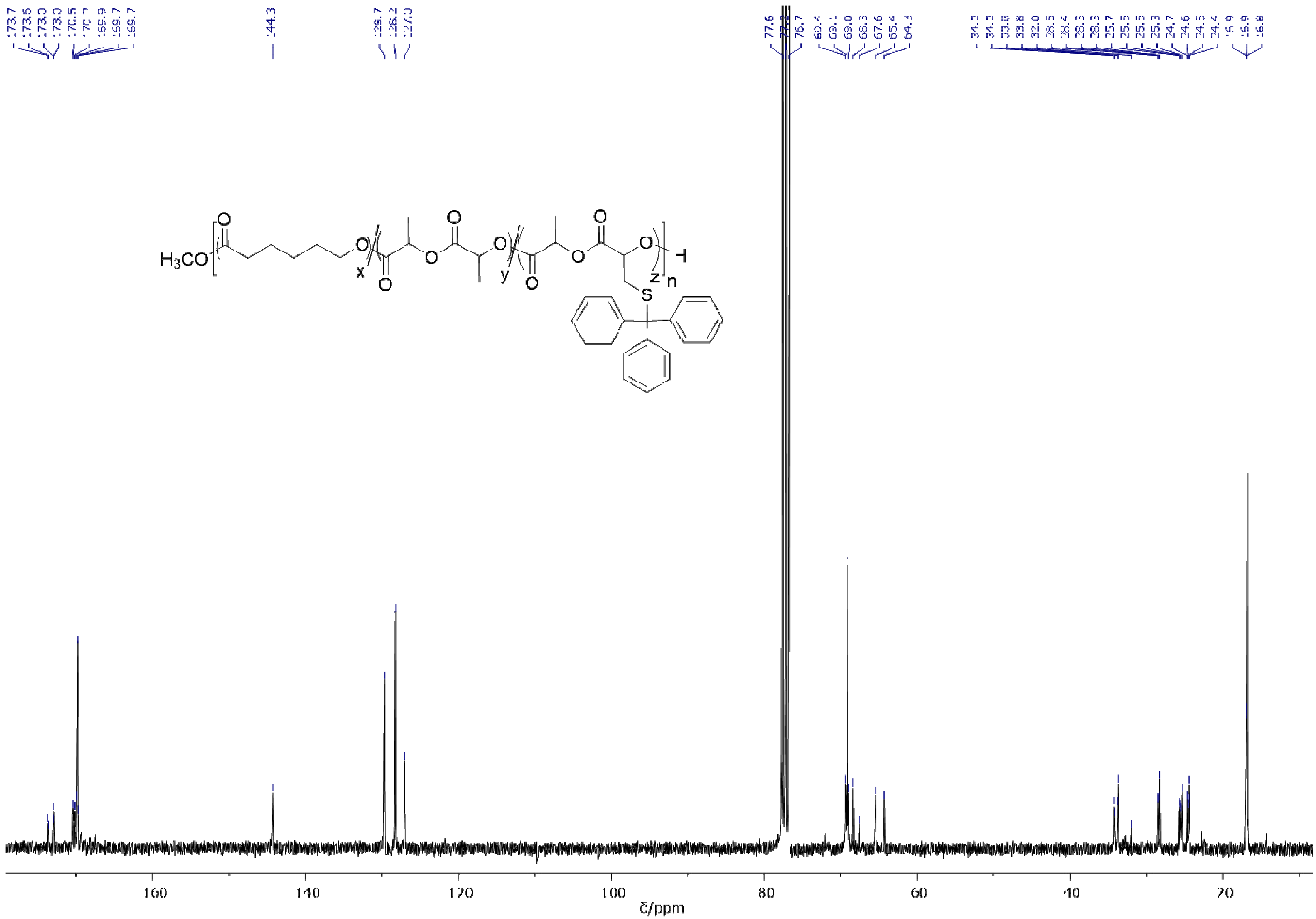

Figure S13. ^{13}C NMR (75 MHz, $CDCl_3$, RT) of poly[(TrtS–LA)-*co*-CL-*co*-LA] (sample **c**).

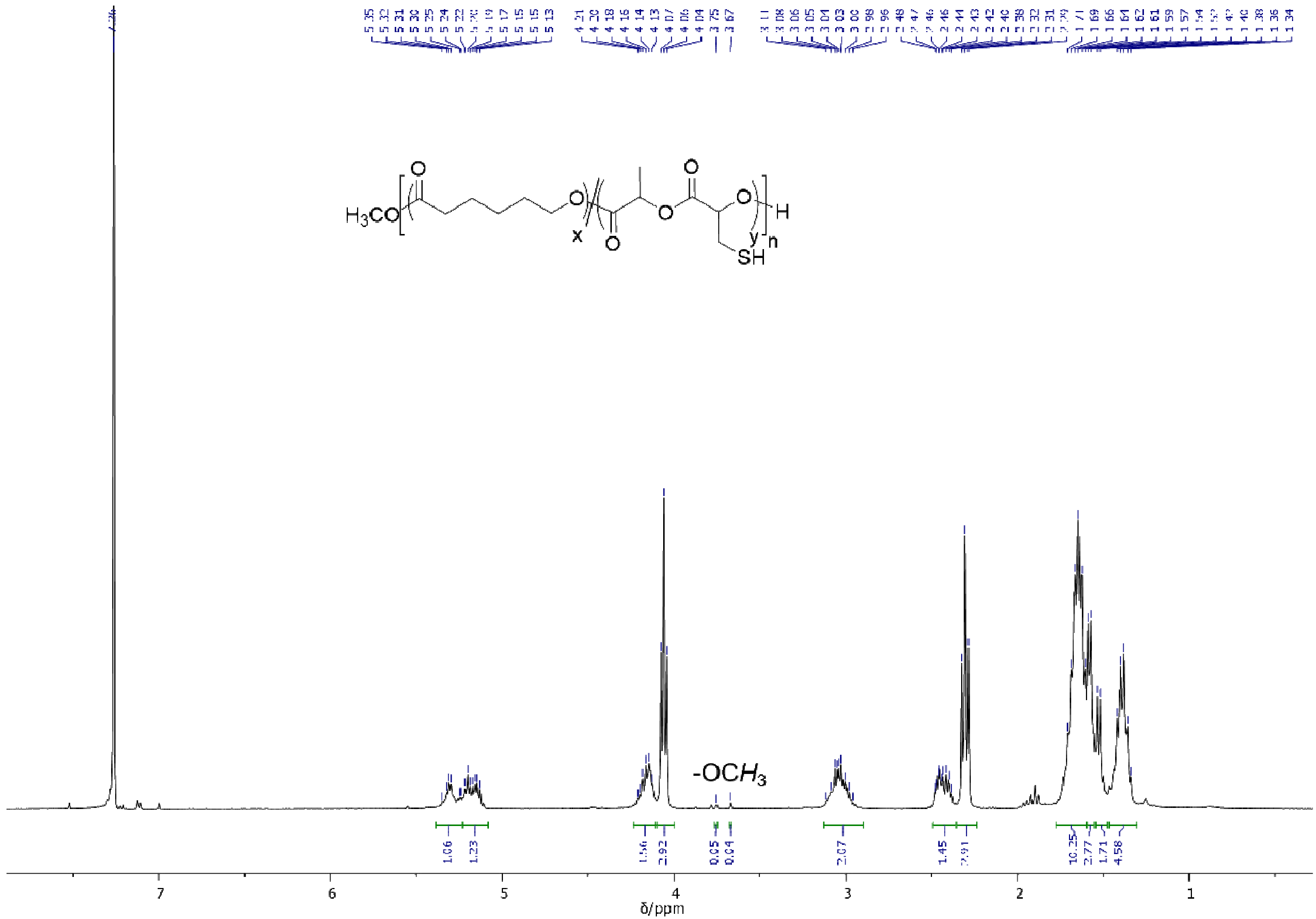

Figure S14. ^{1}H NMR (400 MHz, $CDCl_3$, RT) of poly[(HS–LA)-*co*-CL] (sample **d**).

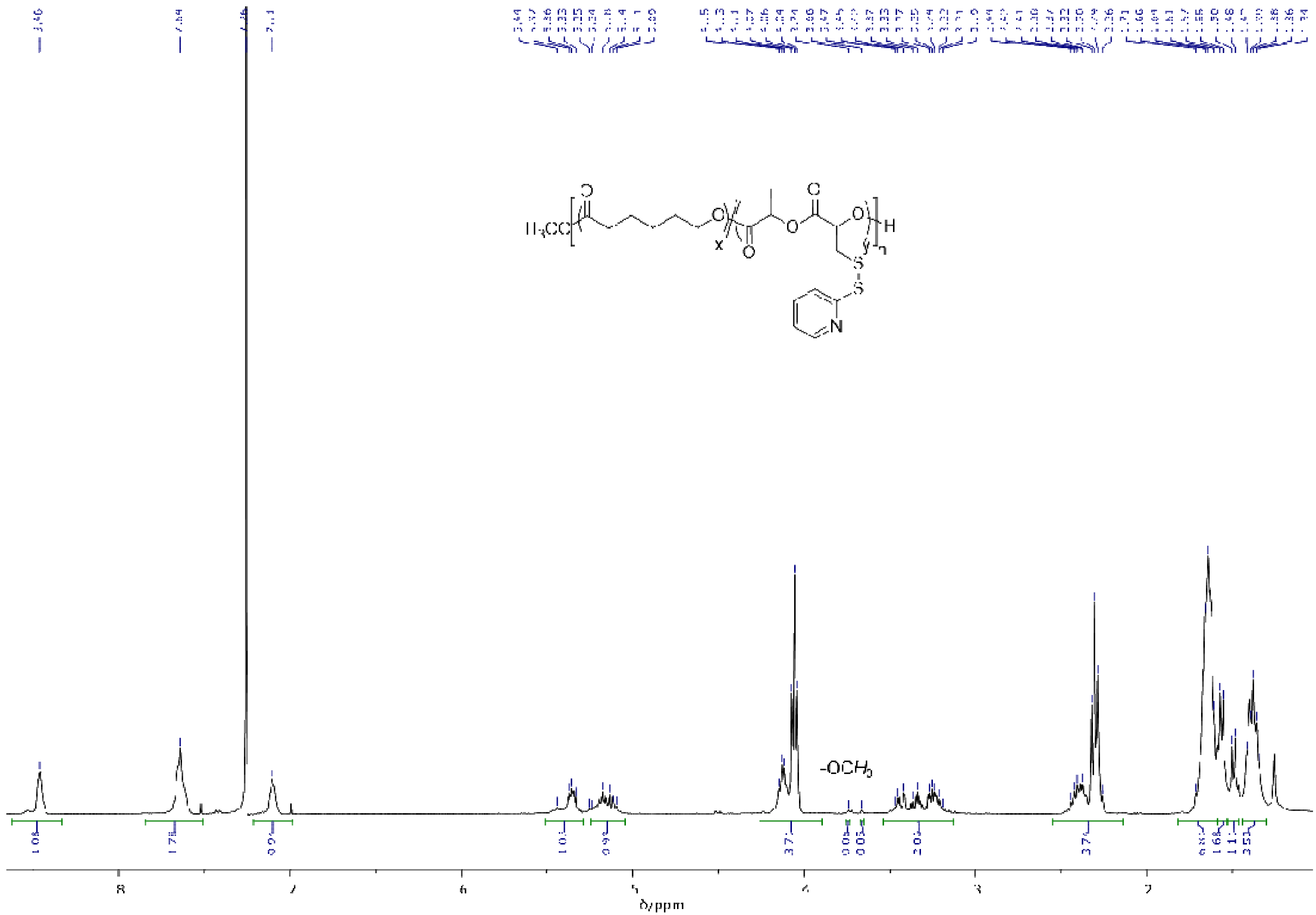

Figure S15. ^{1}H NMR (400 MHz, $CDCl_3$, RT) of poly[(PDS–LA)-*co*-CL] (sample **e**).

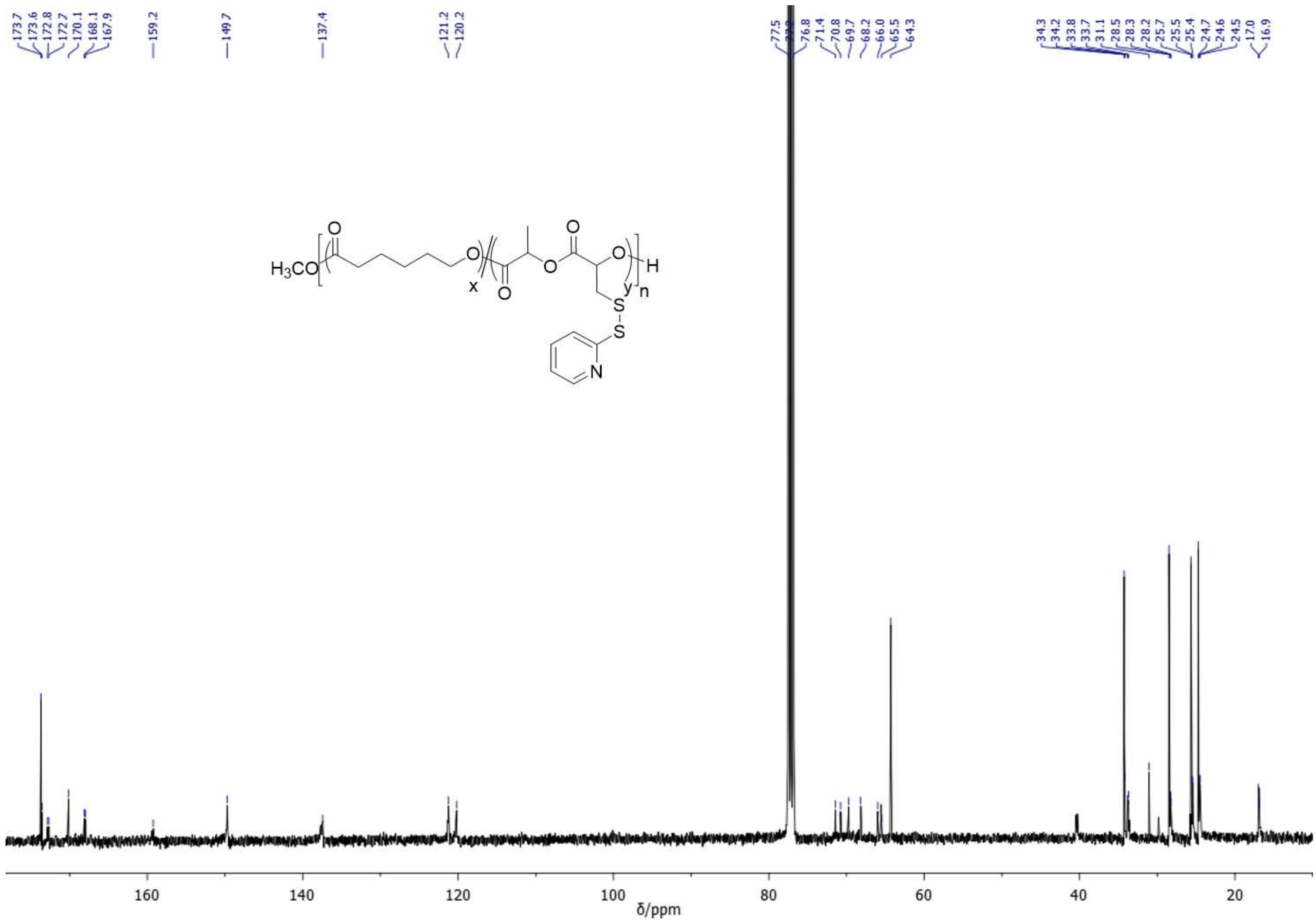

Figure S16. ^{13}C NMR (100 MHz, $CDCl_3$, RT) of poly[(PDS–LA)-*co*-CL] (sample **e**).

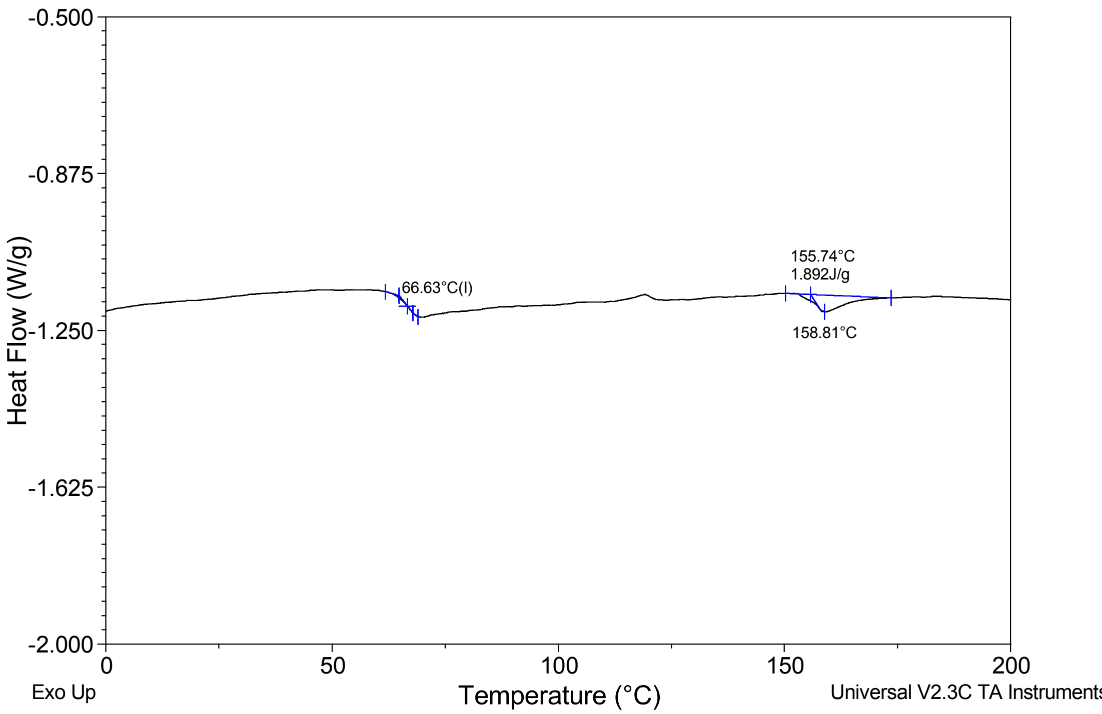

Figure S17. DSC thermogram of poly[(TrtS–LA)-*co*-LA] (sample **a**).

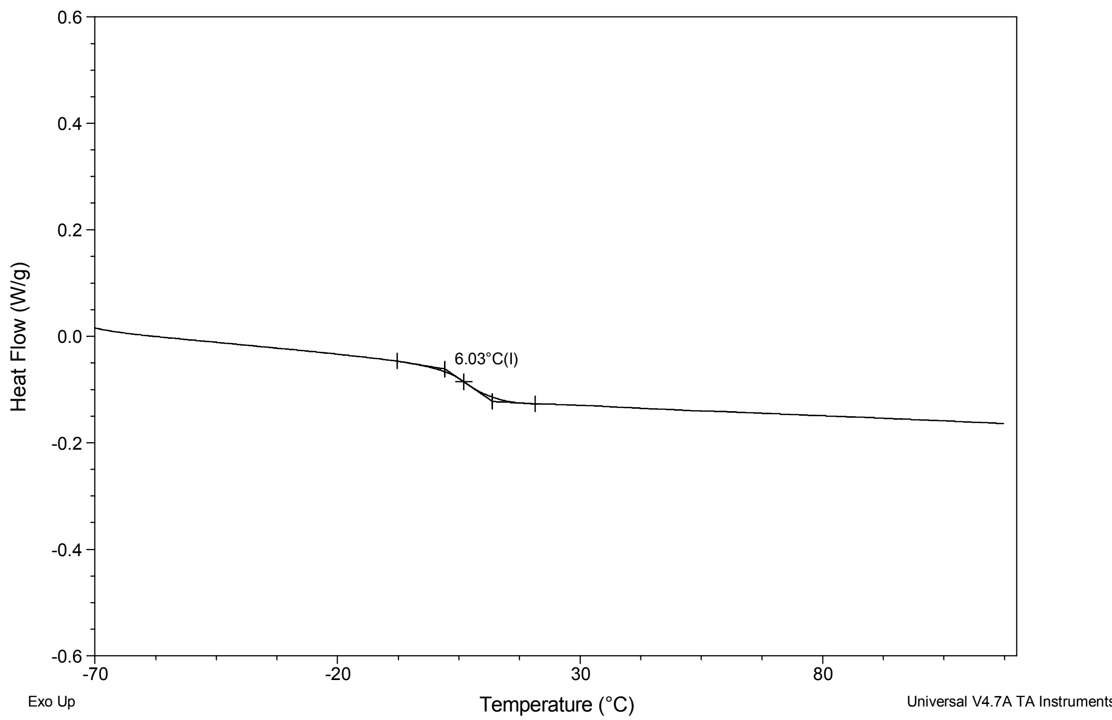

Figure S18. DSC thermogram of poly[(TrtS–LA)-*co*-CL] (sample **b**).

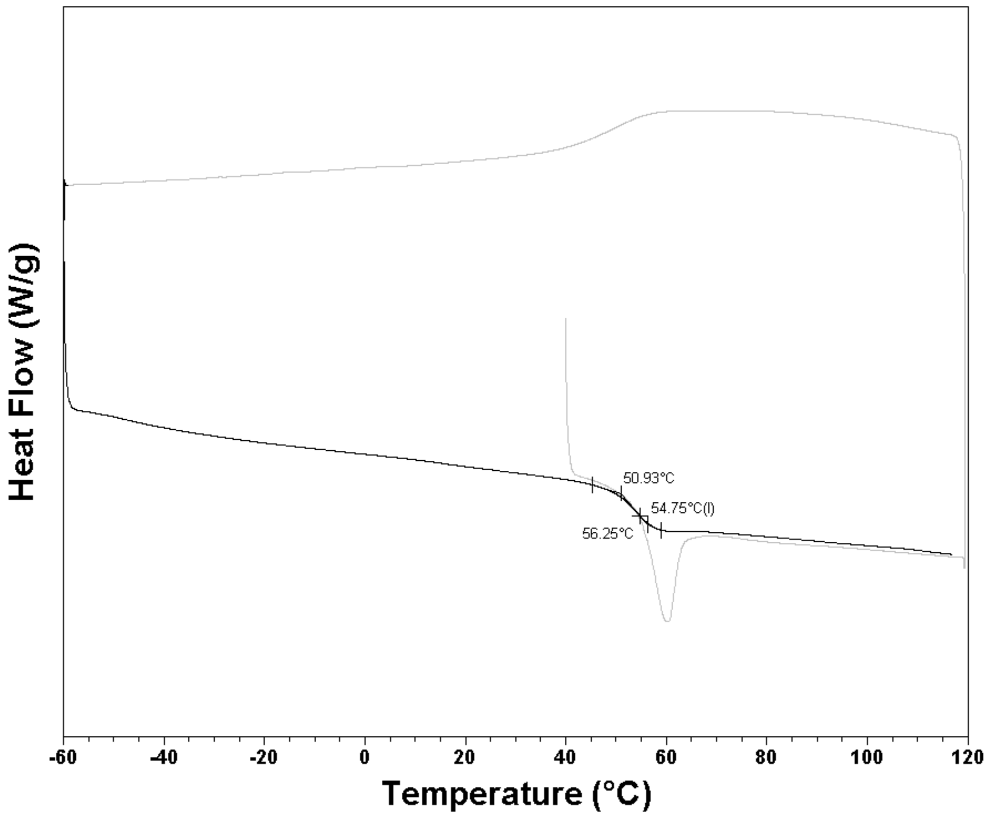

Figure S19. DSC thermogram of poly[(TrtS–LA)-*co*-CL] (sample **b'**).

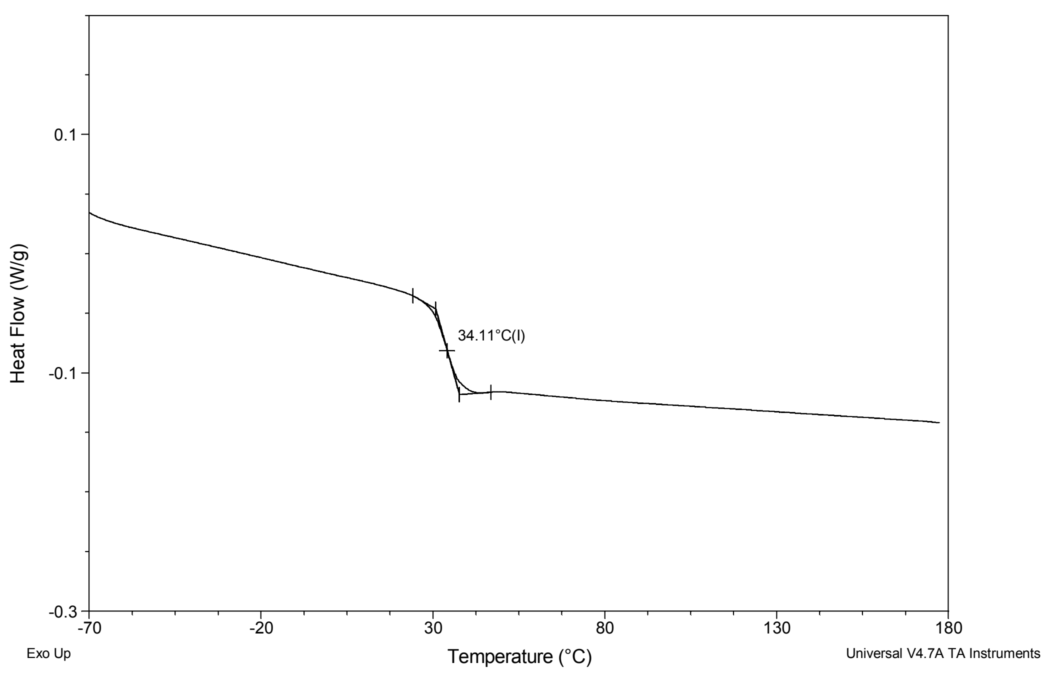

Figure S20. DSC thermogram of poly[(TrtS–LA)-*co*-CL-*co*-LA] (sample **c**).

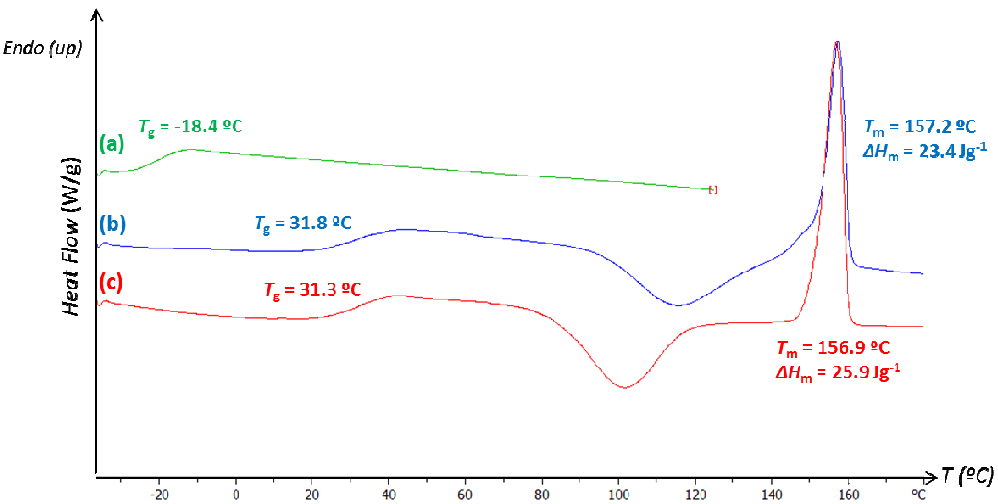

Figure S21. DSC thermograms of: (a) poly[(PDS-LA)-*co*-CL] (green, top); (b) PCLA/ poly[(PDS-LA)-*co*-CL] 90/10 blend (blue, middle); (c) PCLA porous scaffold (red, bottom).

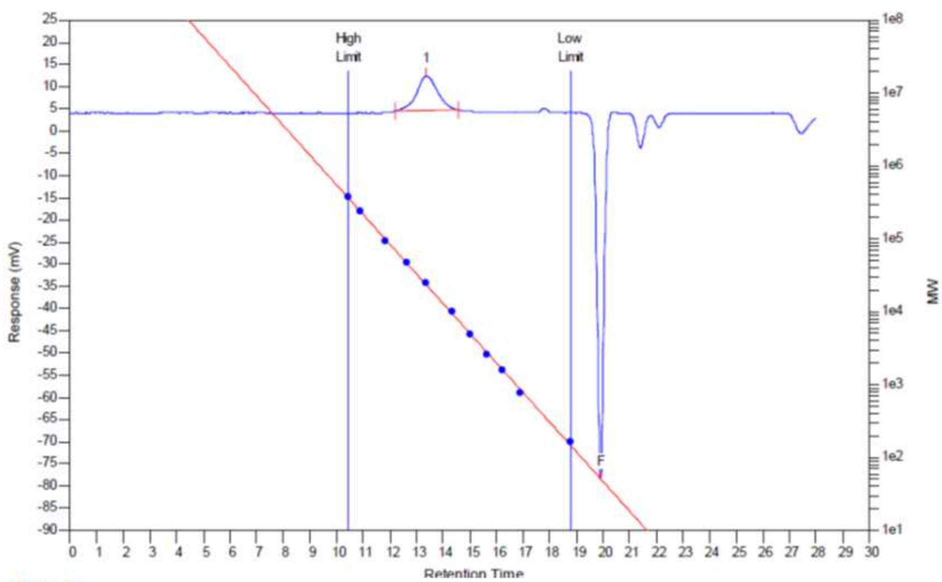

MW Averages

Peak No	Mp	Mn	Mw	Mz	Mz+1	Mv	PD
1	23184	21199	24187	27641	31587	23709	1.14095
2	0	0	0	0	0	0	0

Figure S22. SEC chromatogram of poly[(TrtS–LA)-*co*-LA] (sample **a**).

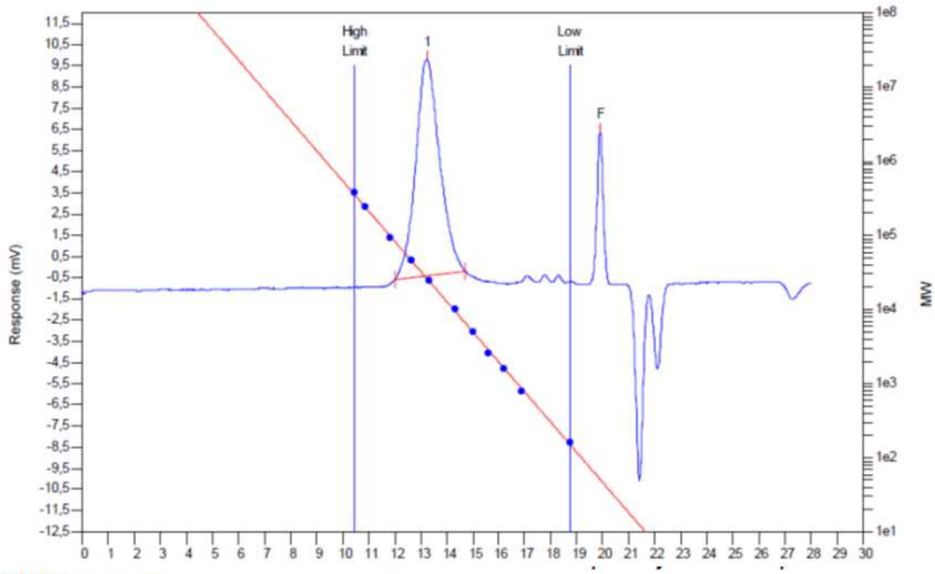

MW Averages

Peak No	Mp	Mn	Mw	Mz	Mz+1	Mv	PD
1	26407	22606	26868	31512	36451	26210	1.18853
2	0	0	0	0	0	0	0

Figure S23. SEC chromatogram of poly[(TrtS–LA)-*co*-CL] (sample **b**).

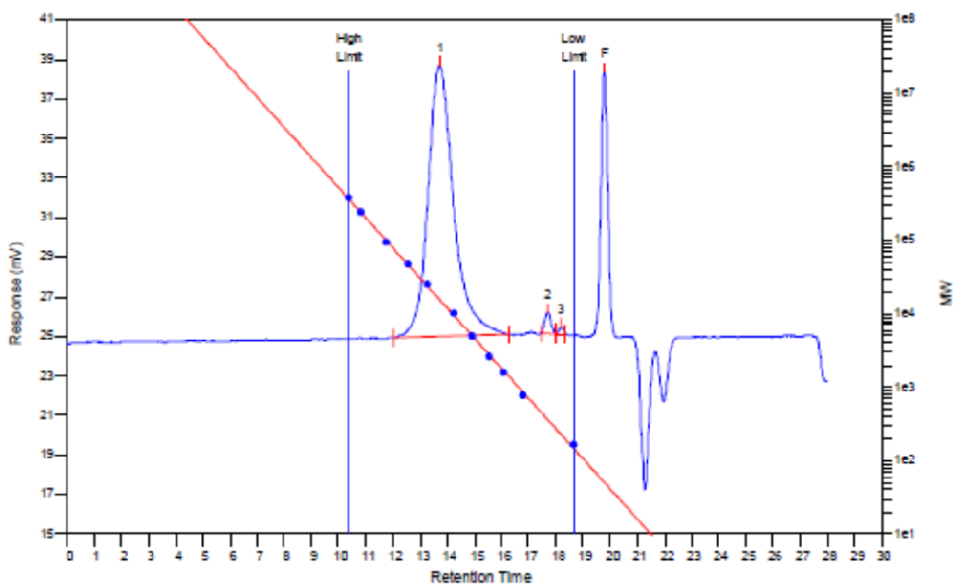

MW Averages

Peak No	Mp	Mn	Mw	Mz	Mz+1	Mv	PD
1	15558	12016	15581	19022	22968	15090	1.29669

Figure S24. SEC chromatogram of poly[(TrtS–LA)-*co*-CL] (sample **b’**).

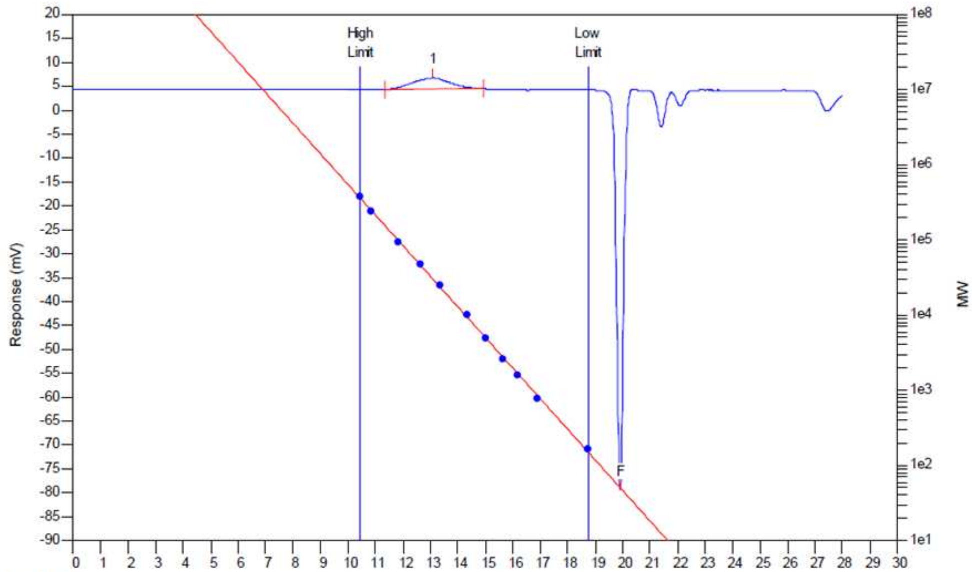

MW Averages

Peak No	Mp	Mn	Mw	Mz	Mz+1	Mv	PD
1	29923	25871	36760	50073	64151	34970	1.4209
2	0	0	0	0	0	0	0

Figure S25. SEC chromatogram of poly[(TrtS–LA)-*co*-CL-*co*-LA] (sample **c**).

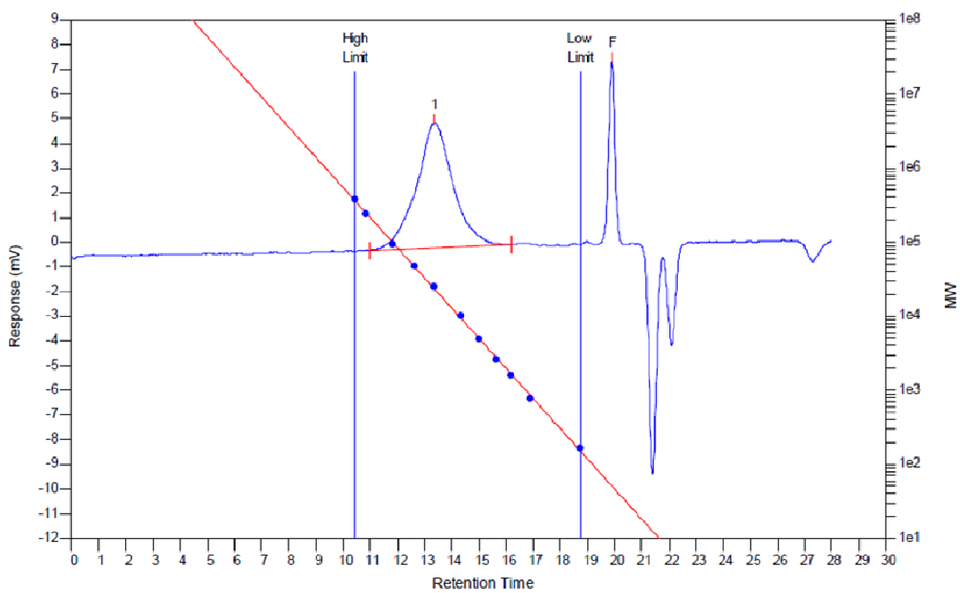

MW Averages

Peak No	Mp	Mn	Mw	Mz	Mz+1	Mv	PD
1	23303	18205	28394	43505	64479	26616	1.55968
2	50	50	51	51	52	51	1.02

Figure S26. SEC chromatogram of poly[(PDS–LA)-*co*-LA] (sample **e**).

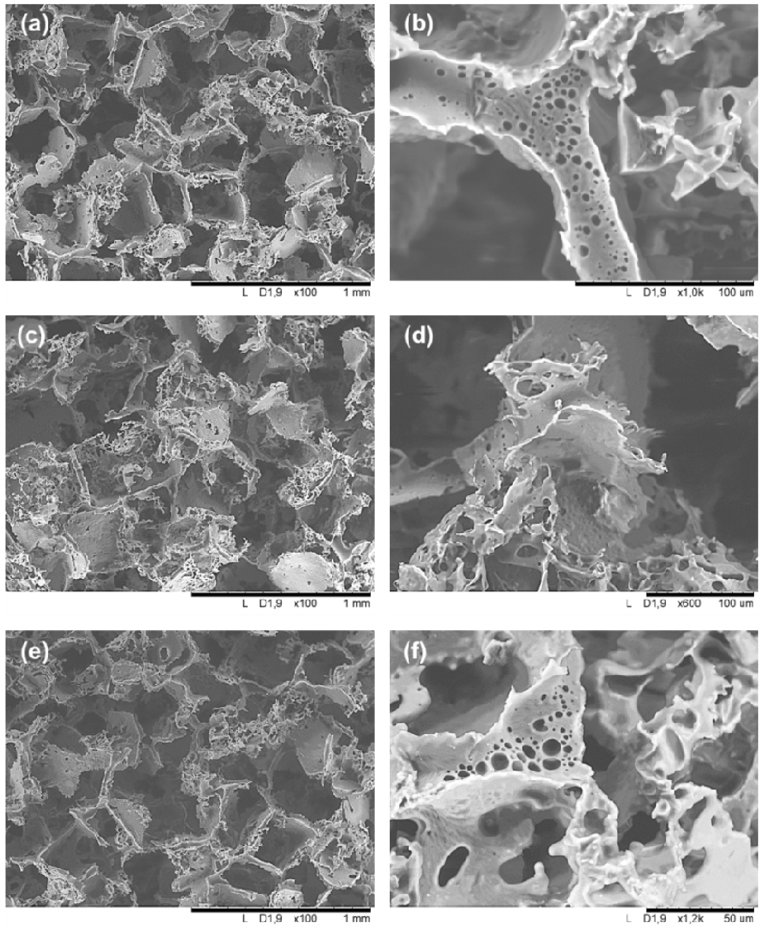

Figure S27. Selected SEM surface images of 3D porous scaffolds of: (a,b) copolymer PCLA; (c,d) poly[(PDS–LA)-*co*-CL]/PCLA 10:90 blend and (e,f) poly[(PDS–LA)-*co*-CL]/PCLA 10:90 blend after RGDC immobilization. Bar lengths are 1 mm (a, c and e); 100 μm (b and d) and 50 μm (f).

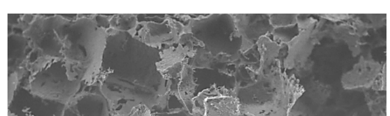

Figure S28. SEM image of the cross-section of a 3D porous scaffolds made with poly[(PDS–LA)-*co*-CL]/PCLA 10:90 blend.

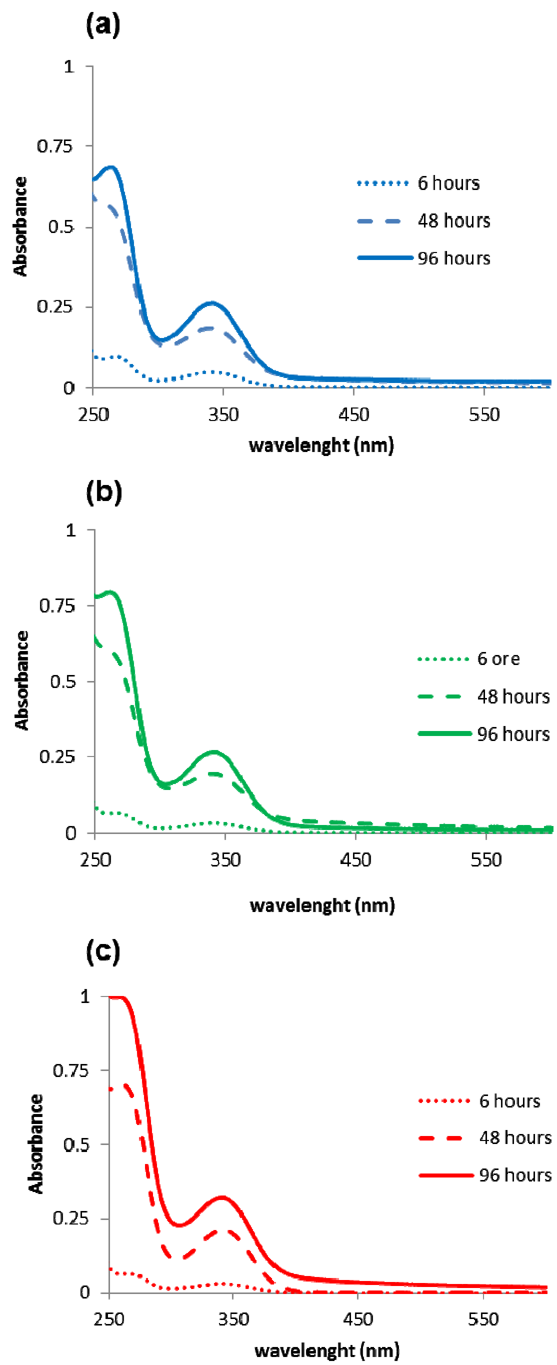

Figure S29. UV spectra of RGDC peptide solution after reaction with porous scaffold having different amount of pyridyl disulfide groups, obtained with a 10/90 (a), 20/80 (b), 30/70 (c) % w/w blends of poly[(PSD–LA)-*co*-CL]/PCLA.

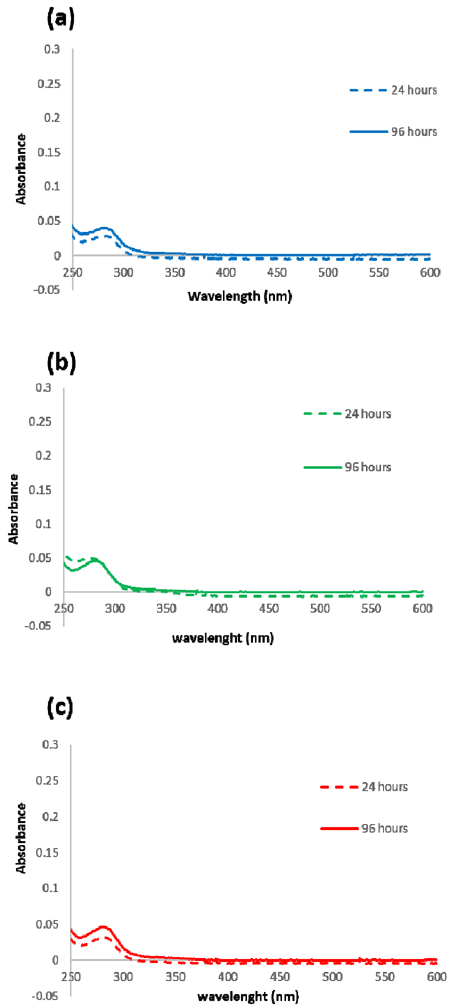

Figure S30. UV spectra of PBS buffered saline after reaction with porous scaffolds obtained with a 10/90 (a), 20/80 (b), 30/70 (c) % w/w blends of poly[(PSD–LA)-*co*-CL]/PCLA.

In detail: three different porous scaffolds (1 mm in thickness and 10 mm in diameter) made by blends of poly[(PDS-LA)-co-CL] and PCLA (10:90; 20:80 and 30:70 % w/w) with contents of pyridyl disulfide groups of 3.4, 4.5 and 6.0 μmol, respectively were used. Porous scaffolds were presoaked in ethanol and then in phosphate-buffered saline (PBS). Afterwards, the scaffolds were soaked with 2.5 mL of PBS. UV spectra (recorded on UV-vis spectrophotometer 2550 over a range of 200-900 nm) of the PBS solutions were recorded at different time (1, 6, 24, 96 hours) to evaluate the released of 2-pyridinethiol. No release of 2-pyridinethiol was observed after 24 hours. After 96 hours the blend poly[(PDS-LA)-co-CL] / PCLA 10:90; 20:80 and 30:70 % w/w released respectively the 0.027, 0.023 and 0.017 % of the 2-pyridinethiol groups.